



Pre-operative magnetic resonance imaging can predict prostate cancer with risk for positive surgical margins

M. Quentin¹ · L. Schimmöller¹ · T. Ullrich¹ · B. Valentin¹ · D. Demetrescu¹ · R. Al-Monajjed² · D. Mally² · I. Esposito³ · P. Albers² · G. Antoch¹ · C. Arsov²

Received: 25 December 2021 / Revised: 21 April 2022 / Accepted: 26 April 2022 / Published online: 16 May 2022
© The Author(s) 2022

Abstract

Purpose Analysis of patients with pre-operative 3 T multiparametric prostate MRI (mpMRI) to determine reliable MRI-based risk predictors of patients at risk for positive surgical margins (PSM) in robotic assisted radical prostatectomy (RPE).

Methods Consecutive patients with 3 T mpMRI and subsequent RPE from 01/2015 to 12/2018 were retrospectively included. Patients were compared regarding clinical and MRI related parameters such as length of capsular tumor contact (LCC) and distance to the membranous urethra (UD).

Results Forty-nine of 179 patients (27%) had PSM in 70 different localizations, with the majority located at the capsule (57%, 40/70), mostly apical and/or posterior. The second most often PSM occurred at the apical urethra (22%, 15/70). PCA was visible on mpMRI at the localization of PSM in 93% at the capsule and in 80% at the urethra. PSA, PI-RADS classification, extraprostatic extension (EPE), and seminal vesicles infiltration (SVI) on MRI were significantly higher / more frequent in patients with PSM. LCC (AUC 0.710), EPE (AUC 0.693), and UD (1-AUC 0.673) predicted PSM (overall). An UD of ≤ 3.5 mm showed the highest accuracy of 95% ($J=0.946$) for PSM at the urethra and a LCC of ≥ 22.5 mm with 77% ($J=0.378$) for PSM at the capsule.

Conclusion PSM occurred mostly in the apex and/or posteriorly at the capsule or at the apical urethra. LCC was the best MRI predictor for PSM at the capsule and UD for tumors with PSM at the apical urethra. Using these MRI parameters readers might pre-operatively determine PCA localizations at risk for PSM.

Keywords Prostate cancer · Prostate MRI · Staging · Prostatectomy · Positive surgical margins · Predictive biomarker

✉ L. Schimmöller
Lars.schimmoller@med.uni-duesseldorf.de

M. Quentin
michael.quentin@gmx.de

T. Ullrich
Tim.Ullrich@med.uni-duesseldorf.de

B. Valentin
Birte.Valentin@med.uni-duesseldorf.de

D. Demetrescu
Doris.Demetrescu@uni-duesseldorf.de

R. Al-Monajjed
Rouvier.Al-Monajjed@med.uni-duesseldorf.de

D. Mally
David.Mally@med.uni-duesseldorf.de

I. Esposito
Irene.Esposito@med.uni-duesseldorf.de

P. Albers
Peter.Albers@med.uni-duesseldorf.de

G. Antoch
Antoch@med.uni-duesseldorf.de

C. Arsov
Christian.Arsov@med.uni-duesseldorf.de

- ¹ Medical Faculty, Department of Diagnostic and Interventional Radiology, University Dusseldorf, Moorenstr. 5, 40225 Dusseldorf, Germany
- ² Medical Faculty, Department of Urology, University Dusseldorf, 40225 Dusseldorf, Germany
- ³ Medical Faculty, Institute of Pathology, University Dusseldorf, 40225 Dusseldorf, Germany

Abbreviations

LCC	Length of capsular tumor contact
EPE	Extraprostatic extension
mpMRI	Multiparametric prostate MRI
PCA	Prostate cancer
PI-RADS	Prostate Imaging Reporting and Data System
PSM	Positive surgical margins
SVI	Seminal vesicle infiltration
UD	PCA distance to the membranous urethra

Introduction

Multiparametric prostate MRI (mpMRI) plays an increasingly significant role in prostate cancer (PCA) diagnostics. Various studies showed that mpMRI is highly sensitive in visualization of PCA suspect lesions and targeted MR-guided biopsy better predict the correct Gleason score on radical prostatectomy (RPE) [1, 2]. Apart from the detection, mpMRI comprises various staging information and is currently seen as the best available imaging tool for assessing extraprostatic extension (EPE) and the T-stage [3–5]. Urologic assessment to predict nonorgan-confined PCA was limited to nomograms based on biopsy results [6]. Meta-analysis showed a moderate sensitivity of 61% of MRI to detect EPE (overall stage T3 disease) with high specificity of 88%, but at 3 Tesla (3 T) MRI also sensitivities above 70% are reported [3, 4]. Over the last year's positron emission tomography (PET) with a prostate specific membrane antigen (PSMA) tracer got higher priority focusing primarily biochemical PCA recurrence and/or M and N staging in high-risk PCA [7–9]. Additional improvement might be achieved by PSMA-PET/MRI and/or artificial intelligence, respectively radiomics [10]. The European Association of Urology (EAU) Guidelines recommend to use pre-biopsy mpMRI for local staging [11].

MRI directed intraoperative frozen-section analysis during nerve-sparing RPE have been shown to reduce the rate of positive surgical margins (PSM) by repeat excision of the tumor at the potential sites of EPE [12]. Nevertheless, PSM also occur in patients with organ-confined PCA. These patients have a higher recurrence rate compared to patients with organ-confined PCA or focal (microscopic) EPE with negative margins [13]. The likelihood of PSM is strongly related with the surgeon's experience independent of the surgical approach [14]. However, while avoiding PSM is the primary goal of RPE, sparing the neurovascular bundles and the membranous urethra is important for continence and potency. Beyond tumor detection and staging, mpMRI provides additional information on anatomy, prostate volume, and tumor localization which could help to identify areas at risk for PSM [15].

Aim of this study was to analyze 3 T mpMRI examinations of patients with subsequent RPE to determine reliable MRI-based risk predictors to identify patients at risk for PSM. Therefore, PCA visibility in PSM localization, length of capsular contact (LCC), EPE, distance to the membranous urethra (UD), and tumor infiltration in other structures was analyzed. The results are supposed to help radiologists to focus on relevant risk predictors and to help urologists with pre-operative planning to avoid PSM.

Materials and methods

Study design

We retrospectively analyzed all consecutive patients from January 2015 to December 2018 with in-house robotic assisted RPE and prior mpMRI for PCA detection ($n = 179$) in this single-center cohort study. We did not include patients without or incomplete mpMRI (Supp. Fig. S1). None of the patients had received prior treatment for PCA. The study was approved by the local Independent Ethics Committee (IEC) (Study number: 2018-227-RetroDEuA; Medical Faculty, University Dusseldorf).

Imaging

The mpMRI of the prostate was performed on a 3 T MRI scanner (Magnetom TIM Trio™, Prisma™ or Skyra™; Siemens Healthineers) with 18 or 60 channel phased-array surface-coils plus/minus 32 channel spine coil according to the European Society of Urogenital Radiology (ESUR) guidelines and the national recommendations [16, 17]. The MR protocol contained T1-weighted images (from the whole pelvis), T2-weighted images (in 3 planes, 3 mm slice thickness), diffusion-weighted images (3 mm slice thickness, b-values: 0, 500, 1000 s/mm² for ADC calculation, an additional high b-value ≥ 1400 s/mm²), and dynamic contrast-enhanced images (DCE; 3 mm slice thickness, scan time 3 min, temporal resolution < 9 s). The detailed MR-protocol has been published previously [18]. All patients received butylscopolamine (20 mg Buscopan®, Boehringer Ingelheim Pharma) to suppress bowel peristalsis.

Image analysis

The mpMRI was retrospectively analyzed by two experienced, board-certified radiologists in consensus subspecialized in prostate MRI (M.Q. and LS, both with more than 10 years' experience in reading prostate MRI) regarding the following aspects in relation to the histopathologic examination of the prostatectomy specimens (localization of positive surgical margins): visible PCA, extraprostatic extension

(EPE), length of capsular tumor contact (LCC), PCA distance to the membranous urethra (UD), and seminal vesicle infiltration (SVI). All measurements were performed on high resolution coronary, sagittal, and/or axial T2-weighted images using the plane that showed the lesion best with reference to DWI (ADC map and high b-value images) and DCE. EPE was defined as extension of the tumor beyond the gland boundary (in mm). LCC was determined by the greatest capsular tumor contact in the different planes using curvilinear measurements along the capsule (in mm). UD was defined as shortest distance of the tumor to the proximal membranous urethra, located between the apex of the prostate and the bulb of the corpus spongiosum, extending through the urogenital diaphragm (in mm). SVI was evaluated if the tumor showed a measurable infiltration of the SV (in mm). PI-RADS classification was performed retrospectively in consensus using PI-RADS version 2.1. Radiologists were blinded to clinical parameters especially PCA aggressiveness, tumor stage, and PSA values.

Prostatectomy

Robotic assisted radical prostatectomy (RPE) was performed with a 3-arm Da Vinci Surgical Si System (Intuitive Surgical) by three different board-certified surgeons (with each more than 10 years' experience) and a transperitoneal access. The decision for curative surgery, as well as decisions for lymph node dissection, was made according to the guidelines of the European Association of Urology [11].

Histopathology was performed according to the recommendations of the International Society of Urological Pathology (ISUP).

Statistical analysis

Descriptive statistics were used to present patient characteristics. Statistical analyses were performed using IBM SPSS® Statistics (Version 21, IBM Deutschland GmbH). Data are expressed as mean \pm SD and median + IQR. Non-parametric Mann–Whitney-U test was used to compare the group of patients with and without PSM. Statistical significance was defined as a p -value < 0.05 . Receiver operating characteristic (ROC) analyses were used for quantifying the impact of clinical and MRI related predictors. Youden index ($J = \text{sensitivity} + \text{specificity} - 1$) was used to measure the clinical diagnostic ability of LCC and UD.

Results

Study population

From 179 included patients, 49 patients had PSM (R1) in at least one localization. The time between MRI and RPE was in mean 12 ± 7.3 weeks. PSA was significant higher in patients with PSM compared to patients without PSM (Table 1). Clinical and postoperative parameters showed limited ability to assess the risk of PSM: age (AUC 0.507; $p = 0.879$), prostate volume (AUC 0.549; $p = 0.315$), PSAD

Table 1 Patient baseline characteristics

		NSM	PSM	<i>P</i> -value*
Clinical data	Patients; number	130	49	
	Age in y; mean \pm SD	66 \pm 8.08	66 \pm 7.95	0.879
	PSA value in ng/ml; median (IQR)	8.84 (6.29 – 12.79)	11 (7.60 – 15.17)	0.006
	PSAD in ng/ml/cm ³ ; median (IQR)	0.23 (0.15 – 0.37)	0.27 (0.22 – 0.40)	0.046
	Prostate volume in ml; median (IQR)	36 (29 – 51)	38 (32 – 50)	0.315
	ISUP; post-biopsy median (IQR)	2 (2 – 3.75)	2 (2 – 4)	0.239
RPE	ISUP; post-surgery median (IQR)	2 (2 – 3)	3 (2–4)	0.031
	T2a-c , % (n)	65% (85)	35% (17)	< 0.001
	T3a , % (n)	22% (28)	24% (12)	
	T3b , % (n)	13% (17)	41% (20)	

*Mann–Whitney-U test

NSM negative surgical margins, PSM positive surgical margins, PSA prostate specific antigen, PSAD prostate specific antigen density, ISUP International Society of Urological Pathology Grade Group

Bold values indicate P -value < 0.05

Table 2 Characterization of lesions with positive surgical margins (PSM)

in % (n)		PSM		
RPE	PSM localization	Side	Left	39% (27/70)
			Right	24% (17/70)
			Both	37% (26/70)
		Capsule	All	57% (40/70)
			Basal	18% (7/40)
			Midgland	27% (11/40)
			Apical	55% (22/40)
			Anterior	35% (14/40)
			Posterior	43% (17/40)
			Lateral	22% (9/40)
			Urethra, apical	22% (15/70)
			SV	14% (10/70)
			Bladder neck	7% (5/70)
			MRI	visible PCA in PSM localization
	LCC 23 ± 12.5 mm (mean \pm SD)			
	EPE	68% (25/37)		
	EPE 4.4 ± 2.1 mm (mean \pm SD)			
	Urethra, apical	80% (12/15)		
	SV	90% (9/10)		
	Bladder neck	100% (5/5)		

PSM positive surgical margins, RPE radical prostatectomy, SV seminal vesicles, EPE extraprostatic extension, LCC length of capsular contact of tumor

Table 3 MRI prediction parameters for positive surgical margins (PSM)

		NSM	PSM	P-value*	
PI-RADS v2.1% (n)	3	3% (4/130)	2% (1/49)	0.002	
	4	43% (56/130)	18% (9/49)		
	5	54% (70/130)	80% (39/49)		
cT3% (n)		72% (107/130)	94% (46/49)	0.040	
EPE % (n)		18% (24/130)	57% (28/49)	< 0.001	
EPE in mm; median (IQR)		3 mm (2 – 5)	4 mm (3 – 6)		
SVI % (n)		9% (12/130)	37% (18/49)	< 0.001	
SVI in mm; median (IQR)		7 mm (5.25 – 11)	8 mm (6 – 11)		
Index lesion	Localization	basal	27% (35/130)	29% (14/49)	0.235
		midgland	33% (43/130)	45% (22/49)	
		apical	40% (52/130)	26% (13/49)	
		anterior	30% (39/130)	37% (18/49)	
		posterior	34% (44/130)	41% (20/49)	
		lateral	36% (47/130)	22% (11/49)	
	LCC in mm; median (IQR)		12 (8 – 18)	20 (13 – 26)	< 0.001
			Cases with PSM at the capsule: 22 (14–28)		
	UD in mm; median (IQR)		15 (12 – 27)	8 (3 – 15)	< 0.001
			Cases with PSM at the urethra: 2 (1–3)		

*Mann–Whitney-U test

NSM negative surgical margins, PSM positive surgical margins, EPE extraprostatic extension, SVI seminal vesicle infiltration, LCC length of capsular contact of tumor, UD distance to the membranous urethra, cT3 clinical T3 stage

Bold values indicate P-value < 0.05

(AUC 0.597; $p=0.05$), PSA (AUC 0.633; $p=0.006$), ISUP grade in biopsy (AUC 0.554; $p=0.264$), ISUP grade after prostatectomy (AUC 0.597; $p=0.05$), with postoperative T-stage being the best parameter (AUC 0.681; $p<0.001$).

Characterization of PSM

PSM were documented in 70 different localizations. The majority of PSM (57%) were located at the capsule, and therein mostly apical and posteriorly (Table 2). The apical urethra was the most infiltrated structure (22%). MpMRI showed a high ability to visualize PCA at the localization of PSM, ranging from 80% at the urethra to 100% at the bladder neck. In 6 patients with PSM the tumor was invisible on mpMRI in the following localizations: 3 at the capsule, one at the seminal vesicles, and in 2 patients at the urethra.

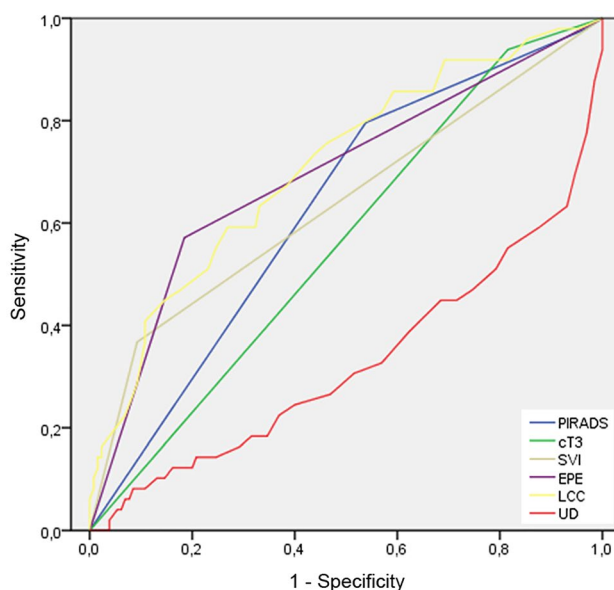
Prediction of PSM

PI-RADS scores were significantly higher in patients with PSM. Also, extraprostatic extension and seminal vesicles infiltration on MRI was significantly more frequent in patients with PSM (Table 3). Index lesions of these patients had a significant higher LCC and a significant lower UD. LCC was the best MRI parameter to predict PSM (AUC 0.710). AUC values for the other MRI parameters were as follows: EPE 0.693, UD 0.327, SVI 0.638, PI-RADS 0.627, and cT3 stage 0.562 (Fig. 1). In the cases with PSM at the apical urethra 1-AUC for UD was 0.981 ($p<0.001$). A UD ≤ 3.5 mm showed highest accuracy with a sensitivity of 100% and specificity of 95% ($J=0.946$) for PSM; a LCC of ≥ 22.5 mm with a sensitivity of 49% and specificity of 89% ($J=0.378$) for PSM at the capsule (Figs. 2, 3 and 4).

Discussion

MpMRI (3 T) showed a high ability to visualize PCA at the localization of PSM, which occurred mostly apical and/or posteriorly at the capsule or at the apical urethra. In 6 patients with PSM the tumor was invisible on mpMRI. 35% of patients with PSM had organ-confined PCA. Best clinical parameter to predict PSM was the postoperative T-stage. LCC was the best MRI predictor for PSM at the capsule, which performed better than the clinical parameters. Nevertheless, in tumors with PSM at the apical urethra, UD was the best MRI parameter. Highest accuracy was documented for UD ≤ 3.5 mm, indicating a high risk for PSM at the urethra and for LCC ≥ 22.5 mm, indicating a high risk for PSM at the capsule. Using these MRI parameters PCA localizations at risk for PSM might be pre-operatively determined.

Park et al. developed and validated a scoring system for MRI to predict PSM inducing the PI-RADS score, tumor



	AUC	Error	p-value	95% CI	
LCC	0.710	0.044	0.000	0.624	0.796
EPE	0.693	0.047	0.000	0.601	0.785
PI-RADS	0.627	0.045	0.009	0.539	0.716
SVI	0.638	0.050	0.005	0.540	0.735
cT3	0.562	0.046	0.204	0.471	0.652
UD	0.327	0.049	0.000	0.231	0.423

Fig. 1 ROC analysis of MRI related predictors for positive surgical margins (PSM). *cT3* clinical T3 stage, *LCC* length of capsular contact of tumor, *EPE* extraprostatic extension, *PI-RADS* Prostate Imaging Reporting and Data System v2.1, *SVI* seminal vesicles infiltration, *UD* PCA distance to the membranous urethra

location on posterolateral side or at the apex, and length of capsular contact, achieving an AUC value of 0.80 [19]. Compared to our results the score was slightly better than LCC alone, but inferior to UD for apical tumors. There are some aspects of this score that needs to be discussed. First, PI-RADS score was weighted more heavily compared to tumor localization. Second, PI-RADS category 3 (clinically significant cancer is equivocal) and PI-RADS category 4 (clinically significant is likely to be present) have the same impact on the score, although in clinical consequence is different. Third, capsular contact ≤ 14 mm was rated with 0. Other studies showed that the risk for EPE was already increased at LCC ≥ 11 mm [4]. Main limitation is that risk factors for PSM depend on the localization of PSM and therefore should be assessed separately for either risk of PSM at the apical urethra or at the capsule.

The diagnostic performance of mpMRI is influenced by the different prevalence of EPE in different risk stratified cohorts [20]. High negative predictive values (88%) are only reached in low-risk cohorts, where patients could benefit if

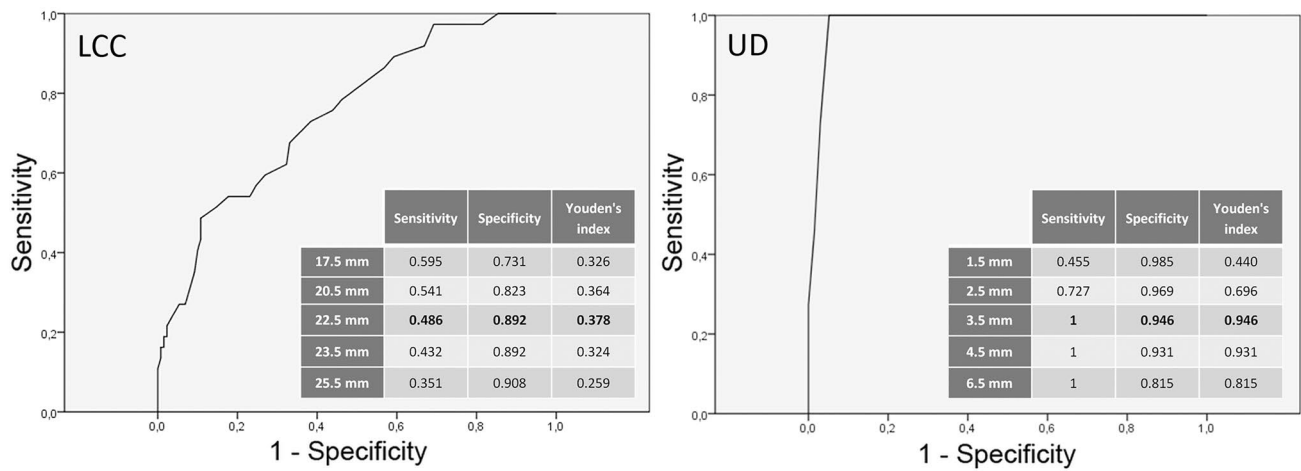
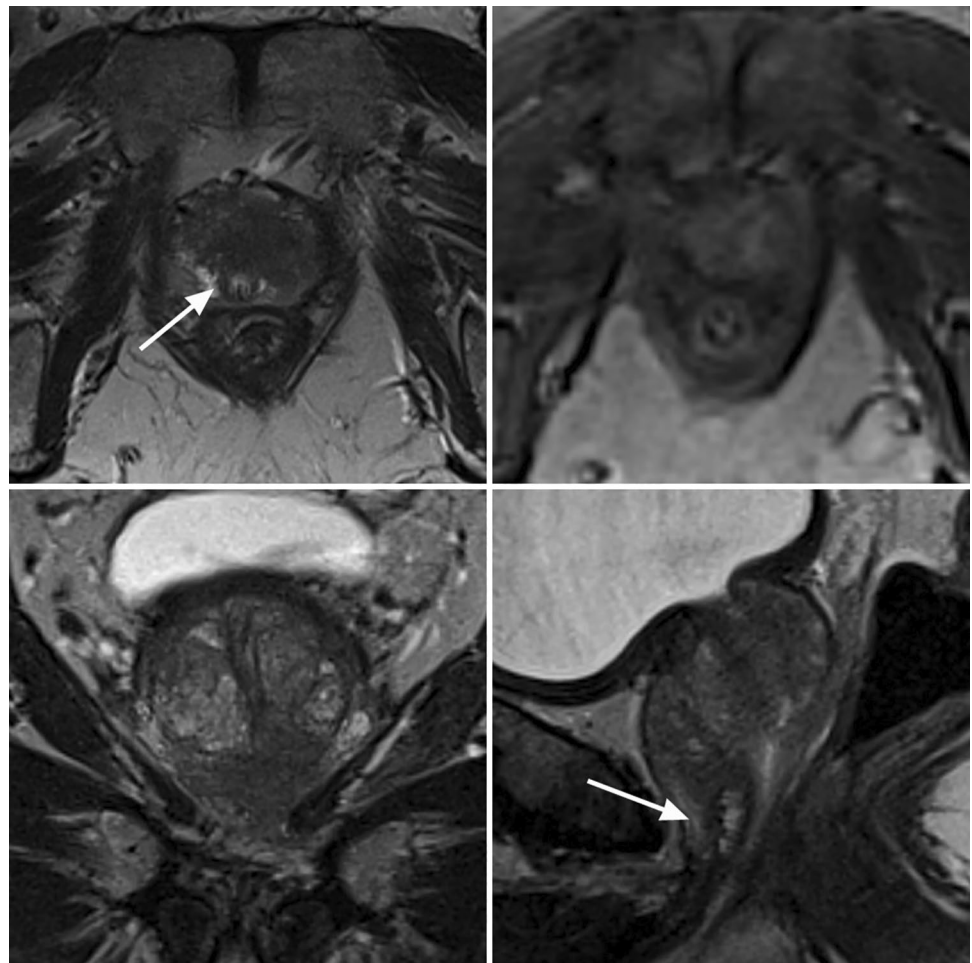


Fig. 2 ROC analysis of LCC as predictor for PSM at the capsule and UD as predictor for positive surgical margin (PSM) at the apical urethra. LCC length of capsular contact of tumor, UD PCA distance to the membranous urethra

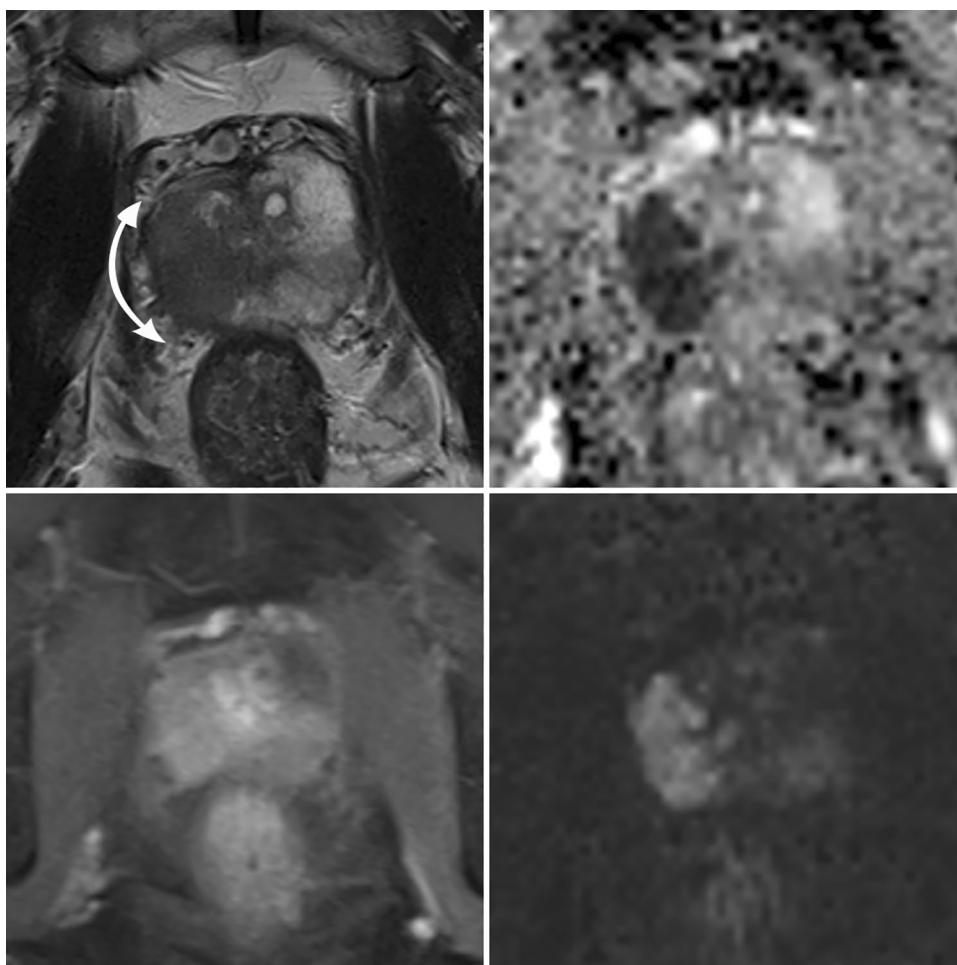
Fig. 3 Patient with organ-confined prostate cancer (T2c) and positive surgical margins at the apical urethra with broad tumor contact to the anterior circumference of the apical urethra on mpMRI. PCA distance to the membranous urethra (UD) was 2 mm (arrows). Upper left: T2 axial, upper right: DCE lower left, T2 coronal, lower right: T2 sagittal



they were selected for nerve sparing surgery by the prior mpMRI. Positive predictive value was highest (89%) in high-risk cohort, which could help to reduce the risk of PSM. In a

prospective randomized single-center trial preoperative MRI could only reduce PSM in low-risk PCA [21]. According to the authors a main limitation is lacking communication

Fig. 4 Patient with extraprostatic extension posterolateral left on mpMRI (T3a) and positive surgical margins in this localization. The length of capsular contact (LCC) of the PCA was 38 mm (double-headed arrow) and extraprostatic extension (EPE) 4 mm. Upper left: T2 axial, upper right: ADC map, lower left: DCE, lower right: high b-value image (b2000)



between radiologists and urologists, which is crucial to adopt surgical approaches.

A recent meta-analysis showed that mpMRI had a considerable impact on the extent of resection during RPE, but modifications of neuro-vascular-bundle preservation did not influence PSM rates [22]. However, apart from relatively small number of studies, mostly retrospective design, different MRI protocols, scanner, and field strength, a further reason for these results might be the lack of standardized MRI reading.

This study is limited by the retrospective design and the single-center evaluation. Although PCA is usually a slow growing tumor, the time interval between MRI and operation might have influenced the results. MRI was acquired at 3 T scanners and reading was performed by subspecialized experts in consensus, but we did not access interreader variability, so less experienced readers may perform differently. Furthermore, PSM at the capsule and at the urethra may have different clinical impact, therapeutic consequence, and risk for biochemical recurrence (BCR). However, this study focuses on the MRI visibility and prediction of PSM.

In conclusion, mpMRI (3 T) was an excellent tool to visualize PCA and could help to identify patients at risk for PSM, which occurs mostly apical and/or posteriorly at the capsule or at the apical urethra. Best predictive parameters were LCC at the capsule and UD for apical located tumors. Since communication with the surgeon is crucial to adopt the surgical strategy, EPE, LCC and UD should be highlighted in the structured report.

Supplementary Information The online version contains supplementary material available at <https://doi.org/10.1007/s00261-022-03543-z>.

Acknowledgements None.

Author contributions Conceptualization: QM, SL, AC, Data curation: QM, SL, DD, MD, EI, AC, Formal analysis: QM, SL, UT, Investigation: SL, UT, VB, MD, EI, Methodology: QM, SL, AC, Project administration: SL, AP, AG, Resources: MD, EI, AP, AG, Software: VB, AR, Supervision: QM, SL, EI, AP, AG, AC, Validation: QM, SL, DD, EI, AG, AC, Visualization: QM, SL, VB, DD, MR, Writing-original draft: QM, SL, Writing-review & editing: SL, UT, AP, AG, AC.

Funding Open Access funding enabled and organized by Projekt DEAL.

Declarations

Conflict of interest There is no conflict of interest. This research did not receive any specific grant from funding agencies in the public, commercial, or not-for-profit sectors.

Open Access This article is licensed under a Creative Commons Attribution 4.0 International License, which permits use, sharing, adaptation, distribution and reproduction in any medium or format, as long as you give appropriate credit to the original author(s) and the source, provide a link to the Creative Commons licence, and indicate if changes were made. The images or other third party material in this article are included in the article's Creative Commons licence, unless indicated otherwise in a credit line to the material. If material is not included in the article's Creative Commons licence and your intended use is not permitted by statutory regulation or exceeds the permitted use, you will need to obtain permission directly from the copyright holder. To view a copy of this licence, visit <http://creativecommons.org/licenses/by/4.0/>.

References

- [1] Thompson JE, Van Leeuwen PJ, Moses D, et al (2016) The diagnostic performance of multiparametric magnetic resonance imaging to detect significant prostate cancer. *J Urol* 195:1428–1435. <https://doi.org/https://doi.org/10.1016/j.juro.2015.10.140>
- Arsov C, Becker N, Rabenalt R, et al (2015) The use of targeted MR-guided prostate biopsy reduces the risk of Gleason upgrading on radical prostatectomy. *J Cancer Res Clin Oncol* 141:2061–2068. <https://doi.org/10.1007/s00432-015-1991-5>
- [3] de Rooij M, Hamoen E, Witjes JA, et al (2016) Accuracy of Magnetic Resonance Imaging for Local Staging of Prostate Cancer: A Diagnostic Meta-analysis. *Eur Urol* 70:233–245. <https://doi.org/10.1016/j.eururo.2015.07.029>
- Valentin B, Schimmöller L, Ullrich T, et al (2021) Magnetic resonance imaging improves the prediction of tumor staging in localized prostate cancer. *Abdom Radiol* 46:2751–2759. <https://doi.org/10.1007/s00261-020-02913-9>
- [5] Valentin B, Arsov C, Ullrich T, et al (2022) Comparison of 3 T mpMRI and pelvic CT examinations for detection of lymph node metastases in patients with prostate cancer. *Eur J Radiol* 147:110110. <https://doi.org/10.1016/j.ejrad.2021.110110>. Epub 2021 Dec 17.
- [6] Pepe P, Frassetto F, Galia A, et al (2008) Is Quantitative Histologic Examination Useful to Predict Nonorgan-Confining Prostate Cancer When Saturation Biopsy Is Performed? *Urology* 72. <https://doi.org/https://doi.org/10.1016/j.urology.2008.05.045>
- [7] Abrams-Pompe RS, Fanti S, Schoots IG, et al (2021) The Role of Magnetic Resonance Imaging and Positron Emission Tomography/Computed Tomography in the Primary Staging of Newly Diagnosed Prostate Cancer: A Systematic Review of the Literature. *Eur Urol Oncol* 4:370–395. <https://doi.org/https://doi.org/10.1016/j.euo.2020.11.002>
- [8] Zhou C, Tang Y, Deng Z, et al. (2022) Comparison of ⁶⁸Ga-PSMA PET/CT and multiparametric MRI for the detection of low- and intermediate-risk prostate cancer. *EJNMMI Res* 12(1):10. <https://doi.org/10.1186/s13550-022-00881-3>.
- [9] Mazrani W, Cook GJR, Bomanji J (2022) Role of ⁶⁸Ga and ¹⁸F PSMA PET/CT and PET/MRI in biochemical recurrence of prostate cancer: a systematic review of prospective studies. *Nucl Med Commun*. <https://doi.org/10.1097/MNM.0000000000001557>.
- [10] Solari EL, Gafita A, Schachoff S, et al. (2022) The added value of PSMA PET/MR radiomics for prostate cancer staging. *Eur J Nucl Med Mol Imaging* 49(2):527–538. <https://doi.org/10.1007/s00259-021-05430-z>
- [11] Mottet N, van den Bergh RCN, Briers E, et al (2021) EAU-EANM-ESTRO-ESUR-SIOG Guidelines on Prostate Cancer—2020 Update. Part 1: Screening, Diagnosis, and Local Treatment with Curative Intent. *Eur Urol* 79:243–262. <https://doi.org/https://doi.org/10.1016/j.eururo.2020.09.042>
- [12] Petralia G, Musi G, Padhani AR, et al (2015) Robot-assisted Radical Prostatectomy: Multiparametric MR Imaging-directed Intraoperative Frozen-Section Analysis to Reduce the Rate of Positive Surgical Margins. *Radiology* 274. <https://doi.org/https://doi.org/10.1148/radiol.14140044>
- [13] Chuang AY, Epstein JI (2008) Positive surgical margins in areas of capsular incision in otherwise organ-confined disease at radical prostatectomy: Histologic features and pitfalls. *Am J Surg Pathol* 32:1201–1206. <https://doi.org/https://doi.org/10.1097/PAS.0b013e318162a8bf>
- [14] Yossepowitch O, Briganti A, Eastham JA, et al (2014) Positive surgical margins after radical prostatectomy: a systematic review and contemporary update. *Eur Urol* 65:303–13. <https://doi.org/https://doi.org/10.1016/j.eururo.2013.07.039>
- [15] McEvoy SH, Raeside MC, Chaim J, et al (2018) Preoperative prostate MRI: A road map for surgery. *Am J Roentgenol* 211:383–391. <https://doi.org/https://doi.org/10.2214/AJR.17.18757>
- [16] Barentsz JO, Richenberg J, Clements R, et al (2012) ESUR prostate MR guidelines 2012. *Eur Radiol* 22:746–757. <https://doi.org/https://doi.org/10.1007/s00330-011-2377-y>
- [17] Franiet T, Quentin M, Mueller-Lisse UG, et al (2017) MRT der Prostata: Empfehlungen zur Vorbereitung und Durchführung. *RoFo Fortschritte auf dem Gebiet der Röntgenstrahlen und der Bildgeb Verfahren* 189:21–28. <https://doi.org/https://doi.org/10.1055/s-0042-119451>
- Schimmöller L, Quentin M, Arsov C, et al (2014) MR-sequences for prostate cancer diagnostics: validation based on the PI-RADS scoring system and targeted MR-guided in-bore biopsy. *Eur Radiol* 24:2582–2589. <https://doi.org/10.1007/s00330-014-3276-9>
- [19] Park MY, Park KJ, Kim M hyun, Kim JK (2021) Preoperative MRI-based estimation of risk for positive resection margin after radical prostatectomy in patients with prostate cancer: development and validation of a simple scoring system. *Eur Radiol* 31. <https://doi.org/https://doi.org/10.1007/s00330-020-07569-z>
- [20] Somford DM, Hamoen EH, Fütterer JJ, et al (2013) The predictive value of endorectal 3 tesla multiparametric magnetic resonance imaging for extraprostatic extension in patients with low, intermediate and high risk prostate cancer. *J Urol* 190:1728–1734. <https://doi.org/https://doi.org/10.1016/j.juro.2013.05.021>
- [21] Rud E, Baco E, Klotz D, et al (2015) Does Preoperative Magnetic Resonance Imaging Reduce the Rate of Positive Surgical Margins at Radical Prostatectomy in a Randomised Clinical Trial? *Eur Urol* 68:487–496. <https://doi.org/https://doi.org/10.1016/j.eururo.2015.02.039>
- [22] Kozikowski M, Malewski W, Michalak W, Dobruch J (2019) Clinical utility of MRI in the decision-making process before radical prostatectomy: Systematic review and meta-analysis. *PLoS One* 14:e0210194. <https://doi.org/https://doi.org/10.1371/journal.pone.0210194>

Publisher's Note Springer Nature remains neutral with regard to jurisdictional claims in published maps and institutional affiliations.